AIP | Journal of Applied Physics

Carrier mobility enhancement in poly(3,4-ethylenedioxythiophene)-poly(styrenesulfonate) having undergone rapid thermal annealing

S. A. Rutledge and A. S. Helmy

Citation: Journal of Applied Physics **114**, 133708 (2013); doi: 10.1063/1.4824104
View online: http://dx.doi.org/10.1063/1.4824104
View Table of Contents: http://scitation.aip.org/content/aip/journal/jap/114/13?ver=pdfcov
Published by the AIP Publishing

Carrier mobility enhancement in poly(3,4-ethylenedioxythiophene)-poly (styrenesulfonate) having undergone rapid thermal annealing

S. A. Rutledge and A. S. Helmy
The Edward S. Rogers Sr. Department of Electrical and Computer Engineering, University of Toronto, Toronto, Ontario M5S 3G4, Canada

(Received 4 July 2013; accepted 17 September 2013; published online 4 October 2013)

The conjugated polymer poly(3,4-ethylenedioxythiophene)-poly(styrenesulfonate) (PEDOT:PSS) is subjected to non-adiabatic rapid thermal processing and exhibits an increase in conductivity through the film. Electrical measurements on an ITO/PEDOT:PSS/Al diode structure display a current-voltage relationship that correlates to space charge limited conduction with the presence of an exponential trap distribution, which is commonly seen in other organic media. With careful application of this current transport theory to the obtained experimental results, the root cause of the conductivity enhancement can be attributed solely to an increase in the charge mobility of carriers in the PEDOT:PSS film. In comparison to an untreated PEDOT:PSS film, processing at 200 °C for 30 s results in a 35% increase in carrier mobility to 0.0128 $cm^2\ V^{-1}\ s^{-1}$. Values for other material characteristics of PEDOT:PSS can also be extracted from this electrical analysis, and additionally are found to be unchanged with processing. Hole concentration, effective density of states, and total trap density are found to be $7.4 \times 10^{14}\,cm^{-3}$, $1.5 \times 10^{18}\,cm^{-3}$, and $3.7 \times 10^{17}\,cm^{-3}$, respectively. © *2013 AIP Publishing LLC*. [http://dx.doi.org/10.1063/1.4824104]

I. INTRODUCTION

The developing maturity of various polymers as effective electronic materials has been motivation to investigate the use of such polymers as a substitute for traditional inorganic materials in various electronic devices ranging from active thin film transistors to passive transparent conducting contacts. Polymer electronic materials offer advantages over their inorganic counterparts thanks to relative material cost, potential for large area deposition, flexibility, while also being light weight and compact.[1] A wide variety of polymers have been investigated for use in electronic devices; however, one of the most promising materials is poly(3,4-ethylenedioxythiophene)-poly(styrenesulfonate) (PEDOT:PSS) due to its excellent conductivity, stability, solubility, and optical characteristics. PEDOT is a conductive, conjugated polymer that after being cross linked with PSS becomes soluble in water. PEDOT:PSS has been investigated for use in a wide variety of applications including thin film transistors, light emitting diodes (LED), photovoltaics (PV), and memory applications.[2–5] While organic materials introduce many exciting alternatives over traditional ones, they do suffer from several limitations including lower carrier mobility, reliability issues, and a limited range of processing temperatures and environments. Various techniques have been developed to enhance PEDOT:PSS conductivity and stability.[6,7] Conventional annealing has been investigated and the results indicate improvements dependent on anneal time, temperature, and atmosphere.[8] Rapid thermal annealing (RTA) has also been applied to thin film PEDOT:PSS and spectroscopic and electrical results have indicated an enhancement of film conductivity parallel to the substrate.[9] RTA is a non-adiabatic annealing process that greatly enhances the heating rate of the sample to modify the sample under non-equilibrium conditions. In particular, RTA has the capabilities to decrease anneal times to be compatible with large area roll-to-roll fabrication techniques. While RTA on inorganic semiconductors has been studied extensively, the effects on polymer materials are not as well developed. Despite the considerable wealth of papers investigating PEDOT:PSS and its continued implementation in organic devices, the conduction mechanism of PEDOT:PSS and current-voltage characteristics are still not fully understood. The aim of this paper is to examine the underlying cause of conductivity enhancement of RTA on PEDOT:PSS as well as investigate the electrical conduction mechanism through the thin polymer film. While spectroscopic material analysis is important in the understanding and development of new and novel materials, the implementation of such functional materials in devices can often result in deviation from the isolated material characteristics. By applying current theoretical understandings of electrical transport in conjugated polymer systems to a hole-only device comprised of ITO/PEDOT:PSS/Al, the understanding of the effects of RTA on PEDOT:PSS have been expanded. In this method, observed conductivity enhancement from RTA can be attributed solely to an increase in carrier mobility, with no marked increase in the values of carrier concentration, effective density of states, and total trap density. In device systems such as organic field effect transistors (OFETs), where material energy levels are critically important for functionality, the tuning and enhancement of carrier mobility without changing material doping and carrier density could lead to improved devices with enhanced performance and reduced power consumption.[10] The capability to extract key material information from electrical measurements in device structures along with being able to tune specific material characteristics while leaving others unchanged will aid in the adaptation and tailoring of future device designs.

II. EXPERIMENTAL

The ITO/PEDOT:PSS/Al devices tested were chosen based on the previous work that has been performed investigating the effects of RTA on PEDOT:PSS and organic device performance.[9] ITO coated boroaluminosilicate slides with a sheet resistivity of 4–10 Ω/□ were purchased from Delta Technologies and cleaned in an O_2 plasma for 5 min to remove any organic materials. PEDOT:PSS, purchased from H. C. Stark under the brand name Clevios F HC, was filtered through a 0.22 μm Micropore filter, then spin cast onto the ITO surface at 2000 revolutions per minute (RPM) for 45 s. A 5 min soft bake at 110 °C was then performed to evaporate any remaining water resulting in a film of thickness of ~100 nm as measured by atomic force microscopy. RTA was then performed with a ramp rate of 25 °C/s followed by a 30 s anneal at either 150 °C, 175 °C, or 200 °C. Al contacts were evaporated into 500 μm^2 pads using a shadow mask resulting in 300 nm film. Lastly, the exposed PEDOT:PSS layer was then removed with an O_2 plasma etch, exposing the ITO substrate.

Electrical DC measurements were obtained with a HP4155 Semiconductor Parametric Analyzer. Testing using a positive applied to both the ITO and the Al pad was performed in order to extract information from the desired material interface with PEDOT:PSS. The testing voltage was limited in order to prevent large current magnitudes, which was found to contribute to significant heating of the ITO substrate and subsequently resulted in gas expulsion and spalling of the PEDOT:PSS film. Figure 1 displays experimental data from an unannealed sample plotted on a log-log scale, in which a positive bias was applied to the Al film, resulting in hole injection from the Al film into the PEDOT:PSS. In Figure 2, the I-V curve is obtained by applying a positive bias to the ITO electrode, corresponding to hole injection from the ITO film into the PEDOT:PSS. Inset in both figures is the correlating linear graph of the higher bias regime. The curve in Figure 2 displays slightly different characteristics as those exhibited with the opposite bias polarity. The interface characteristics in Figure 2, corresponding to hole injection from ITO into PEDOT:PSS, is of most interest due to the fact that it is commonly implemented in current PV and organic light emitting diode (OLED) devices. Various regions have been labeled on the IV curves, which are identified according to the following theoretical model covered in Sec. III.

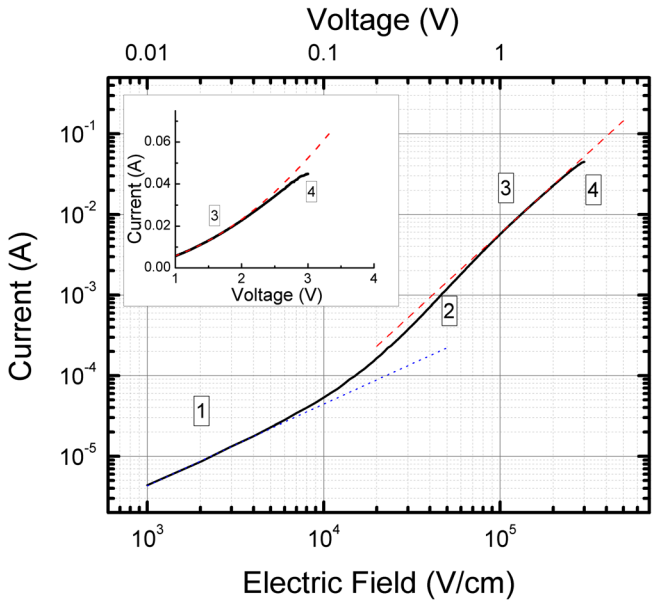

FIG. 1. Logarithmic current-voltage curve of an unannealed hole-only device biased for carrier injection from the Al. Four distinct regions of current-voltage relationship can be identified according to theory. Region 1 at low bias is found to have a linear relation. Region 2 corresponds to space charge limited current with exponentially distributed traps. Region 3 corresponds to space charge limited current beyond the trap filled limit which is related by the well-known V^2 law. In Region 4, the power relationship has dropped below that of the V^2 law and is beginning to tend towards a second linear region at high voltages due to the occurrence of a Schottky barrier between the Al and the PEDOT:PSS. For reference, the dotted line is a fit to an ohmic relation at low voltages, and the dashed line is a fit to the V^2 law. It can be observed that the slope of experimental curve drops below that dotted line at high biases. (Inset) A linear graph of the experimental curve and simulated V^2 law curve in the higher voltage regime.

III. DISCUSSION

A. Extracting material parameters from electrical results

Analyzing the type of electrical contact between the PEDOT:PSS and the electrode materials is critical for device implementation. In the ITO/PEDOT:PSS/Al sandwich structure developed, the band structure of the device can be modeled as seen in Figure 3. The work functions of ITO and PEDOT:PSS range from 4.2–4.7 to 4.8–5.4 eV, respectively, dependent on material processing, while Al is known to have a work function of ~4.3 eV.[7,11]

Taking into account that PEDOT:PSS is a hole transporting material and that the work function of ITO and Al are both less than that of PEDOT:PSS, there is an expected energy barrier to overcome for carriers to be injected into the PEDOT:PSS film. Conversely, there is no barrier for hole extraction at the either contact, and is therefore assumed to be ohmic.

1. Theory of current transport through organic medium

The mechanisms of current transport through organic media have been under investigation for many years. The current understanding of the J-V behavior of organic diodes follows a trap-filling model in which three distinct regions of current transport can be modeled. At low voltages transport follows ohmic behavior as outlined in Eq. (1):[12]

$$J = qp\mu\frac{V}{d}, \tag{1}$$

where J is the current density through the device, q is the elementary charge, p is the volume density of holes, μ is the carrier mobility of carriers (assuming single carrier transport), V is the applied voltage, and d is the thickness of the organic layer.

At moderate voltages, the J-V relationship increases as the space charge limited current (SCLC) dominates and is controlled by distributed traps within the material according to Eq. (2).[12,13]

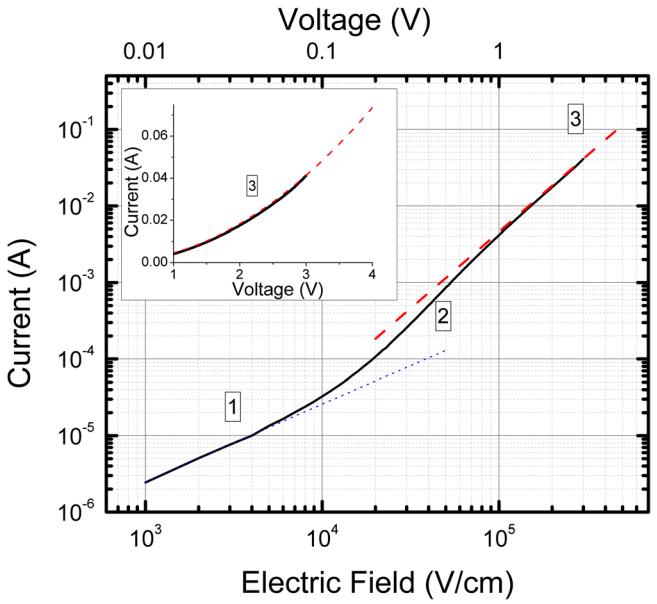

FIG. 2. Logarithmic current-voltage curve of an unannealed hole-only device biased for carrier injection from the ITO. Three distinct regions of current-voltage relationship can be identified according to theory. Region 1 at low bias is found to have a linear relation. Region 2 corresponds to space charge limited current with exponentially distributed traps. Region 3 corresponds to space charge limited current beyond the trap filled limit which is related by the well-known V^2 law. For reference, the dotted line is a fit to an ohmic relation at low voltages, and the dashed line is a fit to the V^2 law at high biases. It can be seen that the experimental curve never falls below the slope of the dotted reference line at any applied bias. (Inset) A linear graph of the experimental curve and simulated V^2 law curve in the higher voltage regime.

$$J = q^{l-1}\mu N_V \left(\frac{2l+1}{l+1}\right)^{l+1} \left(\frac{l}{l+1}\cdot\frac{\varepsilon}{H_b}\right)^{l} \cdot \frac{V^{l+1}}{d^{2l+1}}. \quad (2)$$

In the above equation, N_V is the density of states in the valence band of the organic material, H_b is the total trap density, $\varepsilon = \varepsilon_r\varepsilon_0$, where ε_r is the relative permittivity of the organic and ε_0 is that of free space, $l = T_C/T$, where T_C is the characteristic temperature of an exponential trap distribution in the material.

At even higher applied voltages, the current transitions again and exhibits the commonly seen V^2 law, given by Eq. (3).[12,13]

$$J = \frac{9}{8}\varepsilon\mu\frac{V^2}{d^3}. \quad (3)$$

However, the SCLC equations given in Eqs. (2) and (3) have been further refined by Kumar *et al.* to take into account non-ohmic injection interface between the injecting contact and the organic material.[14] At sufficiently high voltages, due to the fact that the concentration of holes at the injecting contact is not infinitely large is assumed in the derivation of Eq. (3), the power relationship between current and voltage will subsequently decay back to a linear relationship.

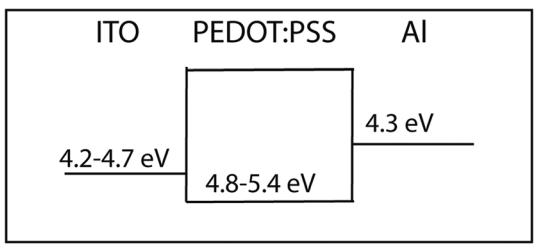

FIG. 3. Schematic of the energy levels of ITO, PEDOT:PSS, and Al in the devices fabricated.

2. Fitting experimental results to theory

Applying the discussed theoretical model to the IV experimental data and depending on the polarity of the applied bias, differences in current-voltage characteristics can be observed between carrier injection from either the ITO or the Al.

Identified on the curve in Figure 1, corresponding to carrier injection from the Al contact, are four distinct regions of current conduction characteristics. Region 1 is a linear region at low bias corresponding to Eq. (1), which is extrapolated for reference using a dotted line. Region 2 is the trap filling SCLC in which the current increases at a level higher than predicted by the V^2 law in Eq. (2). Region 3 is the regime where SCLC in the absence of traps is evident (a dashed line has been plotted according to the traditional V^2 law), prior to the onset of Region 4, in which the curve can be seen to drop below a squared power at a sufficiently high bias due to the injection energy barrier between Al and PEDOT:PSS.

Applying Eq. (2) to the corresponding Region 3, values for the carrier mobility can be extracted, under the assumption that the relative permittivity of PEDOT:PSS is ~2.2. Figure 4(a) displays the average of carrier mobility with respect to annealing temperature, and can be seen to increase by a factor of almost 35% from the unannealed value of 0.0095 $cm^2\ V^{-1}\ s^{-1}$ up to 0.0128 $cm^2\ V^{-1}\ s^{-1}$ with annealing at 200 °C. These values are of similar magnitude to those recently reported as determined through testing in a FET structure.[15]

Similar current-voltage regions can be identified correlating to the low voltage ohmic relationship (Region 1) and the trap filled SCLC relationship (Region 2). While the ITO heating during device operation again limited the maximum bias, a significant difference when compared to injection from the Al contact is that the device cannot be biased far enough to display a drop below, or even to the V^2 law, as was previously observed. With the previously determined hole mobility as determined from the Al injection results, values of carrier concentration in the PEDOT:PSS film (p) can be obtained through fitting to Eq. (1) in the low voltage linear regime and the values are graphically depicted in Figure 4(b).

In a similar manner, by applying Eq. (2) to the appropriate biasing range, the number available density of states (N_V) and values for total trap density (H_b) can be acquired and are shown in Figures 4(c) and 4(d), respectively. It is noted that while the carrier mobility of PEDOT:PSS was seen to increase with annealing temperature, the other material parameters were virtually unaffected. This enhanced mobility and subsequent conductivity is consistent with the previous results that indicated the modification of the

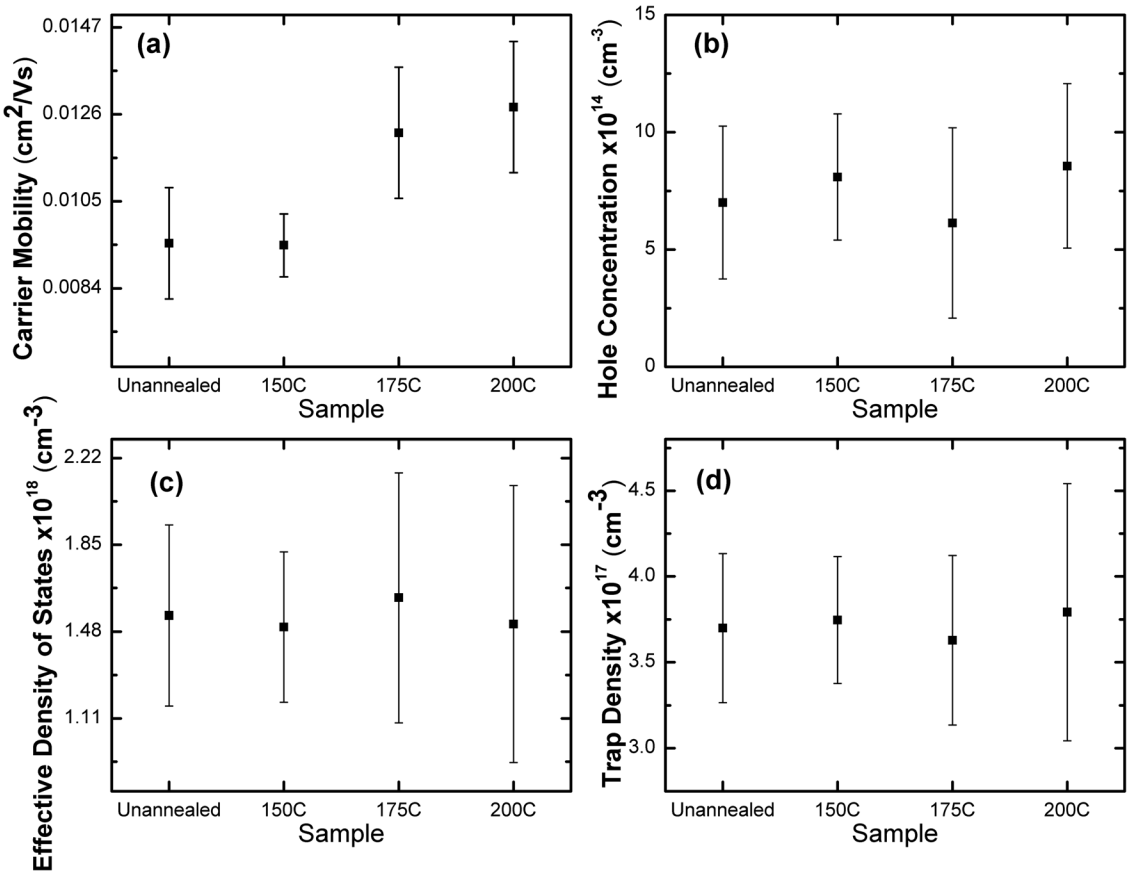

FIG. 4. Results from fitting the theoretical current-voltage equations to experimentally obtained data. Error bars indicate the standard deviation of several devices tested in the same fabrication. (a) Displays values of hole mobility (μ) in the PEDOT:PSS with respect to RTA temperature. (b) Displays values of hole concentration (p) in the PEDOT:PSS with respect to RTA temperature. (c) Displays values of the effective density of states in the PEDOT:PSS (N_V) with respect to RTA temperature. (d) Displays values of the total trap density (H_b) of the PEDOT:PSS with respect to RTA temperature.

structure of PEDOT:PSS film allowing for enhanced mobility of charge carriers along the polymer chain backbone.[9] Also available from these results are approximate values for the hole concentration of PEDOT:PSS of 7.4×10^{14} cm^{-3}, density of valence states of 1.5×10^{18} cm^{-3}, and total trap density of 3.7×10^{17} cm^{-3}.

B. Impact of RTA effects on device properties

Organic heterojunctions, with either organic materials or inorganic ones, are obviously of key importance for device implementation. The material characteristics that have been extracted (carrier mobility, carrier concentration, effective density of states, and total trap density) are all critically important to organic thin film devices. Energy level engineering through material doping, material mobility, and the effect of trap distribution on charge conduction are continually investigated and play vital roles in OFETs and OLEDs functionality, power consumption, and transport characteristics.[16,17] From this analysis, several key observations as to the effects of the RTA on the ITO/PEDOT:PSS/Al device can be made. Primarily, that with increasing annealing temperature, the hole mobility in PEDOT:PSS is increased. This expands further on the previously observed results dealing with the application of RTA to PEDOT:PSS thin films and is able to elucidate the hole mobility enhancement as the sole factor of increased conductivity through the film.[9] Often the role of implementing PEDOT:PSS into a PV or OLED structure is as a hole transport layer, or conducting electrode based on its energy level alignment with respect to other materials in the system. Enhancing PEDOT:PSS conductivity is desirable in such devices to lower power consumption through unwanted series resistance. By utilizing RTA as a post-growth processing technique, the resistivity of PEDOT:PSS is lowered. Of key importance is the fact that the conductivity increase is found to be solely due to the increase of carrier mobility, and not of carrier concentration from material doping. Adjusting material doping, while increasing conductivity, would otherwise additionally change the Fermi energy level in polymer materials. This could potentially disrupt the energy level engineering and matching with subsequent layers in a device stack. RTA could potentially be used in complement to chemical doping of PEDOT:PSS, to enhance mobility without changing the desired material energy levels. In OFETs, carrier mobility of channel materials is again of critical importance to operating voltage and power consumption, and the capability to isolate processing effects to only adjust material mobility will allow for increased flexibility of design. While the manipulation of density of states and total trap density has not been demonstrated in this investigation, both play an important role in determining the relationship between current transport and

applied bias through organic materials. The non-varying values extracted from this analysis provide a basis for precise device modeling and enhanced characterization of polymer devices implementing PEDOT:PSS layers. The consistent nature of these material characteristics with RTA temperature allows for precise tuning of carrier mobility, without disrupting other characteristics of the material that could otherwise adjust the current-voltage relationship.

IV. CONCLUSION

While PEDOT:PSS is a widely used in PV and OLED applications, its current transport behaviour is still not sufficiently characterized, and often either ohmic behaviour is assumed or the PEDOT:PSS is regarded as being the injecting contact material. From this analysis, we are able to observe similar current transport behaviour as identified in other conducting polymer devices, with a linear relation between current and voltage at low biases, followed by a trap filling space charge limited region, and then once the traps in PEDOT:PSS have been sufficiently filled, the traditional SCLC V^2 relationship. The effects of an energy barrier to hole injection from Al into PEDOT:PSS are seen to limit the SCLC behaviour at sufficiently high voltages, and it might also be expected that a similar barrier would be observed due to injection from the ITO contact. However, due to material heating constraints, such bias levels were unavailable. Combined with this new insight into current transport through PEDOT:PSS, a modest increase in hole mobility, and subsequent conductivity, of 44% can be realized with rapid thermal processing at 200 °C for only 30 s. Aside from the increase of hole mobility, RTA has no discernible effect on values of PEDOT:PSS carrier concentration, total trap density, and effective density of states. The unique effects of RTA increasing only carrier mobility while leaving other material characteristics unchanged, and additionally the ability to realize such enhancement in a very short processing time, offers an effective post-growth thin film processing technique compatible with roll-to-roll deposition technology.

[1]S. R. Forrest, Nature **428**, 911 (2004).
[2]X. Crispin, F. L. E. Jakobsson, A. Crispin, P. C. M. Grim, P. Anderrsson, A. Volodin, C. van Haesendonck, M. van der Auweraer, W. R. Salaneck, and M. Berggren, Chem. Mater. **18**, 4354 (2006).
[3]H. S. Kang, H.-S. Kang, J. K. Lee, J. W. Lee, J. Joo, J. M. Ko, M. S. Kim, and J. Y. Lee, Synth. Met. **155**, 176 (2005).
[4]Y. Kim, A. M. Ballantyne, J. Nelson, and D. D. C. Bradley, Org. Electron. **10**, 205 (2009).
[5]J. Wang, X. Cheng, M. Caironi, F. Gao, X. Yang, and N. C. Greenham, Org. Electron. **12**, 1271 (2011).
[6]S. K. M. Jönsson, J. Birgeson, X. Crispin, G. Greczynski, W. Osikowicz, A. W. D. van der Gon, W. R. Salaneck, and M. Fahlman, Synth. Met. **139**, 1 (2003).
[7]A. M. Nardes, M. Kemerink, M. M. de Kok, E. Vinken, K. Maturova, and R. A. J. Janssen, Org. Electron. **9**, 727 (2008).
[8]J. Huang, P. F. Miller, J. C. de Mello, A. J. de Mello, and D. D. C. Bradley, Synth. Met. **139**, 569 (2003).
[9]A. A. Farah, S. A. Rutledge, A. Schaarschmidt, R. Lai, J. P. Freedman, and A. S. Helmy, J. Appl. Phys. **112**, 113709 (2012).
[10]S. Allard, M. Forster, B. Souharce, H. Thiem, and U. Scherf, Angew. Chem., Int. Ed. **47**, 4070 (2008).
[11]J. S. Kim, M. Granström, R. H. Friend, N. Johansson, W. R. Salaneck, R. Daik, W. J. Feast, and F. Cacialli, J. Appl. Phys. **84**, 6859 (1998).
[12]A. J. Campbell, D. D. C. Bradley, and D. G. Lidzey, J. Appl. Phys. **82**, 6326 (1997).
[13]S. C. Jain, A. K. Kapoor, W. Geens, J. Poortmans, R. Mertens, and M. Willander, J. Appl. Phys. **92**, 3752 (2002).
[14]P. Kumar, S. C. Jain, V. Kumar, S. Chand, and R. P. Tandon, Eur. Phys. J. E **28**, 361 (2009).
[15]Q. Wei, M. Mukaida, Y. Naitoh, and T. Ishida, Adv. Mater. **25**, 2831 (2013).
[16]P. E. Burrows, Z. Shen, V. Bulovic, D. M. McCarty, S. R. Forrest, J. A. Cronin, and M. E. Thompson, J. Appl. Phys. **79**, 7991 (1996).
[17]S. Scheinert and G. Paasch, Phys. Status Solidi **201**, 1263 (2004).